

Article

# Voltammetric Sensing of Chloride Based on a Redox-Active Complex: A Terpyridine-Co(II)-Dipyrrromethene Functionalized Anion Receptor Deposited on a Gold Electrode

Kamila Malecka-Baturo <sup>1</sup>, Mathias Daniels <sup>2</sup>, Wim Dehaen <sup>2</sup>, Hanna Radecka <sup>1</sup>, Jerzy Radecki <sup>1,†</sup> and Iwona Grabowska <sup>1,\*</sup>

<sup>1</sup> Institute of Animal Reproduction and Food Research, Polish Academy of Sciences, Tuwima Street 10, 10-748 Olsztyn, Poland; k.malecka@pan.olsztyn.pl (K.M.-B.); h.radecka@pan.olsztyn.pl (H.R.)

<sup>2</sup> Sustainable Chemistry for Metals and Molecules, Department of Chemistry, KU Leuven, Leuven Chem&Tech, Celestijnenlaan 200F, B-3001 Leuven, Belgium; wim.dehaen@kuleuven.be (W.D.)

\* Correspondence: i.grabowska@pan.olsztyn.pl

† Deceased.

**Abstract:** A redox-active complex containing Co(II) connected to a terpyridine (TPY) and dipyrrromethene functionalized anion receptor (DPM-AR) was created on a gold electrode surface. This host-guest supramolecular system based on a redox-active layer was used for voltammetric detection of chloride anions in aqueous solutions. The sensing mechanism was based on the changes in the redox activity of the complex observed upon binding of the anion to the receptor. The electron transfer coefficient ( $\alpha$ ) and electron transfer rate constant ( $k_0$ ) for the modified gold electrodes were calculated based on Cyclic Voltammetry (CV) experiments results. On the other hand, the sensing abilities were examined using Square Wave Voltammetry (SWV). More importantly, the anion receptor was selective to chloride, resulting in the highest change in Co(II) current intensity and allowing to distinguish chloride, sulfate and bromide. The proposed system displayed the highest sensitivity to  $\text{Cl}^-$  with a limit of detection of 0.50 fM. The order of selectivity was:  $\text{Cl}^- > \text{SO}_4^{2-} > \text{Br}^-$ , which was confirmed by the binding constants ( $K$ ) and reaction coupling efficiencies ( $RCE$ ).

**Keywords:** voltammetric sensor; anion recognition; host-guest interaction; terpyridine-Co(II)-dipyrrromethene complex; chloride sensing



**Citation:** Malecka-Baturo, K.; Daniels, M.; Dehaen, W.; Radecka, H.; Radecki, J.; Grabowska, I. Voltammetric Sensing of Chloride Based on a Redox-Active Complex: A Terpyridine-Co(II)-Dipyrrromethene Functionalized Anion Receptor Deposited on a Gold Electrode. *Molecules* **2024**, *29*, 2102. <https://doi.org/10.3390/molecules29092102>

Academic Editor: Antonella Curulli

Received: 7 March 2024

Revised: 16 April 2024

Accepted: 29 April 2024

Published: 2 May 2024



**Copyright:** © 2024 by the authors. Licensee MDPI, Basel, Switzerland. This article is an open access article distributed under the terms and conditions of the Creative Commons Attribution (CC BY) license (<https://creativecommons.org/licenses/by/4.0/>).

## 1. Introduction

The quantitative detection of anions is more challenging than that of cations due to their high hydration energy, complex geometry and pH-dependent properties [1,2]. Anionic species play a significant role in many chemical, biological, industrial, medical and environmental processes [3]. Therefore, the selection of appropriate detection techniques is in high demand [4]. Many analytical techniques, including absorption spectroscopy, fluorescence spectroscopy and electroanalytical methods, have been applied for sensing anions [5–7]. On the other hand, electrochemical sensors, including voltammetric, impedimetric, capacitive and potentiometric methods, thanks to their low price, sensitivity and scalability, have received increasing attention [7–12]. Most of these sensors contain synthetic receptors capable of reversibly binding anions based on non-covalent interactions, in particular hydrogen and halogen bonds [13]. These receptors could be immobilized on the surface of solid electrodes with recognition processes occurring at the solid/aqueous interface. In such a case, redox-active species could be either added to the sample solution [14] or functionalized with anion receptors and deposited on a solid substrate [15]. However, the development of electrochemical systems enabling the detection of anions in aqueous solutions, which consist of anion receptors linked in proximity with redox-active sites, is still of interest to the research community. The host-guest recognition phenomenon

in such systems demands electrochemical communication between anion receptors and redox-active sites [16]. The binding mechanism between an anion receptor-bearing redox transducer and anions and subsequent signal transduction is still not fully understood [15].

Electrochemical sensors for the detection of chloride, thanks to their portability, relatively low cost, fast detection and user-friendliness, have the potential to be adjusted for on-site detection. Some voltammetric, potentiometric and colorimetric chloride sensors have been developed recently [17]. Just as an example, compact discs were used for preparation of working, counter and pseudo-reference electrodes and were set up in a three-electrode configuration cell, followed by using linear scan voltammetry (LSV) with a limit of detection (LOD) for chloride ions of 20  $\mu\text{M}$ . In this case, excellent selectivity and reproducibility were reported [18]. Another chronoamperometric sensor for the detection of chloride ions was based on multiwalled carbon nanotubes (MWCNT), silver nanoparticles (AgNPs) and hydrophilic copper benzene 1,3,5-tricarboxylate (Cu-BTC) deposited on a flexible polytetrafluoroethylene (PTFE) substrate [19]. The electrochemical sensing of chloride has also been reported on glassy carbon electrodes (GCE) modified with AgNPs decorated into cavities of a zeolitic imidazolate framework 8 (ZIF-8). The reported sensor showed excellent stability, reproducibility and selectivity towards chloride ions with a LOD of 0.61  $\mu\text{M}$  [20]. All of these examples concern the use of silver-based electrodes to detect  $\text{Cl}^-$ . Another type of sensor is based on three screen-printed electrodes (SPE): a working, an auxiliary (both carbon paste electrodes, CPEs), and a pseudo-reference Ag/AgCl paste-based electrode. The carbon paste of the working SPE was filled with potassium ferricyanide, potassium ferrocyanide and ferrocenemethanol (FcMeOH). The systematic shift of the voltammetric peak potential of FcMeOH upon contact with chloride ions displayed the lowest LOD of 10 mM for  $\text{Cl}^-$  [21]. The LOD was further improved for this system using Gore-Tex<sup>®</sup> support, up to 0.2 mM for chloride ions [22]. The systems in which redox-active species are co-immobilized together with anion receptors on the solid substrate and the detection of anions occurring in water are scantily present in the literature [23]. Several reports have been presented by the group of Beer and co-workers [7,15], but these systems were studied in non-aqueous solutions.

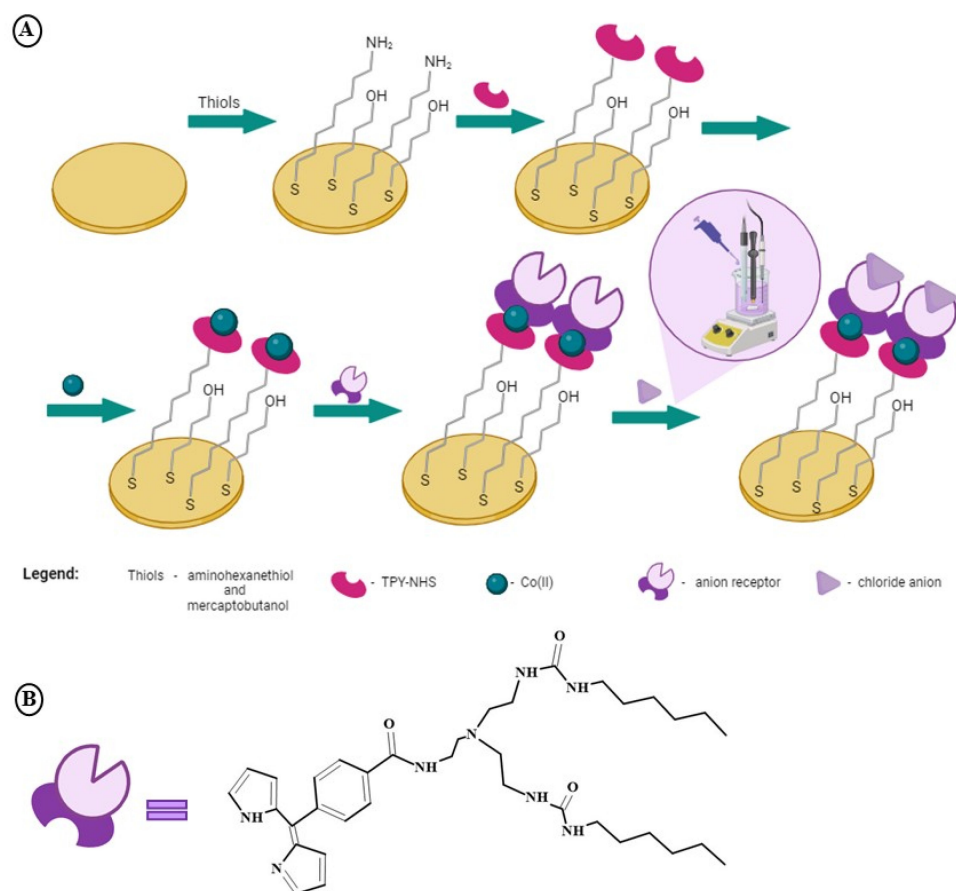
In our previous work, we proposed an electrochemical anion sensor made of electroactive dipyrromethene (DPM) complexes with Co(II) or Cu(II) incorporating anion receptor (AR), deposited onto a gold electrode ((Au/DPM/Co(II), Cu(II)/DPM-AR)) [23]. This system is based on a bifunctional receptor composed of receptor-binding sites and redox-active centers. The binding of anions to receptor molecules influences changes in electron transfer reactions, which is the basis of the generation of the analytical signal. Based on the previously obtained results, we can conclude that Co(II) redox centers showed better selectivity towards  $\text{Cl}^-$  than Cu(II) centers. In the present work, we have tested terpyridines as a possible coordination ligand [24]. The complexes of Co(II) with TPY and a dipyrromethene functionalized anion receptor (DPM-AR) were deposited on a gold electrode for sensing  $\text{Cl}^-$  using SWV. The chloride ions are very common in the environment due to intensive human industrial activity. High chloride content is dangerous to human life; therefore, it is important to carefully monitor the chloride content in water. There is a need to develop new methodologies that are characterized by high sensitivity, high throughput and high anti-interference ability [25]. Our system offers ultra-high sensitivity for chloride anions, with a detection limit of 0.5 fM. Therefore, the innovation of the system presented is related to the possibility of detecting these anions in very diluted samples, which can possibly reduce the matrix effect (possible interferences).

## 2. Results and Discussion

### 2.1. The Procedure of Au/MBL, AHT/TPY/Co(II)/DPM-AR Layer Preparation

The sensing layer was prepared based on a step-by-step gold electrode modification procedure. The first step was to simultaneously immobilize 6-amino-1-hexanethiol (AHT) and 4-mercapto-1-butanol (MBL) onto a gold electrode. In this way, the amino groups were available to create a covalent bond with TPY-bearing N-hydroxysuccinimide (NHS) groups.

Upon complexation of TPY with Co(II) cations, DPM-AR molecules were attached to the electrode as the final step. An illustration of the redox-active sensing layer preparation (Au/MBL, AHT/TPY/Co(II)/DPM-AR) is presented in Scheme 1A. The chemical structure of the DPM-AR is shown in Scheme 1B. The system developed in this way contains a bifunctional receptor composed of a Co(II) redox-active center and an anion receptor. As a result of molecular recognition between the anion receptor and a specific anion, changes in the electrochemical activity of the redox-active Co(II) centers are registered by electrochemical methods, which are the base of the generation of the analytical signal. The bare gold electrodes were electrochemically characterized before modification. The electroactive surface area ( $A_{\text{eas}}$ ) and the roughness factor ( $RF$ ) were determined, which were  $0.32 \pm 0.02 \text{ cm}^2$  and  $10.34 \pm 0.52$ , respectively (Equations (S1)–(S3), Supplementary Materials) [26,27].



**Scheme 1.** (A) Schematic representation of the gold electrode modification with the redox-active layer and anion receptor; (B) Structure of the anion receptor (DPM-AR).

## 2.2. The Electrochemical Characterization of the Au/MBL, AHT/TPY/Co(II)/DPM-AR Layer

The Au/MBL, AHT/TPY/Co(II)/DPM-AR redox-active layer was initially electrochemically characterized by CV experiments conducted at different scan rates from 0.05 to 1.0 V/s in a 0.1 M NaNO<sub>3</sub> + 0.01 M H<sub>3</sub>BO<sub>3</sub> buffer at pH 4.0 (Figure 1A). The composition and pH of the supporting electrolyte were thoroughly optimized in our previous studies [23]. At the scan rate of 0.1 V/s, the reduction and oxidation peaks were registered at the potentials of  $309 \pm 11 \text{ mV}$  and  $383 \pm 16 \text{ mV}$ , respectively. These results therefore demonstrate quasi-reversible electrode reactions for Co(II) deposited on the gold electrode surface. On the other hand, the linear relationships of reduction and oxidation peak currents vs. scan rate confirm the presence of Co(II) centers on the surface of the gold electrodes (Figure 1B). The cathodic peak is more pronounced, so the slope of the cathodic peak current was larger than the slope of the anodic peak current.

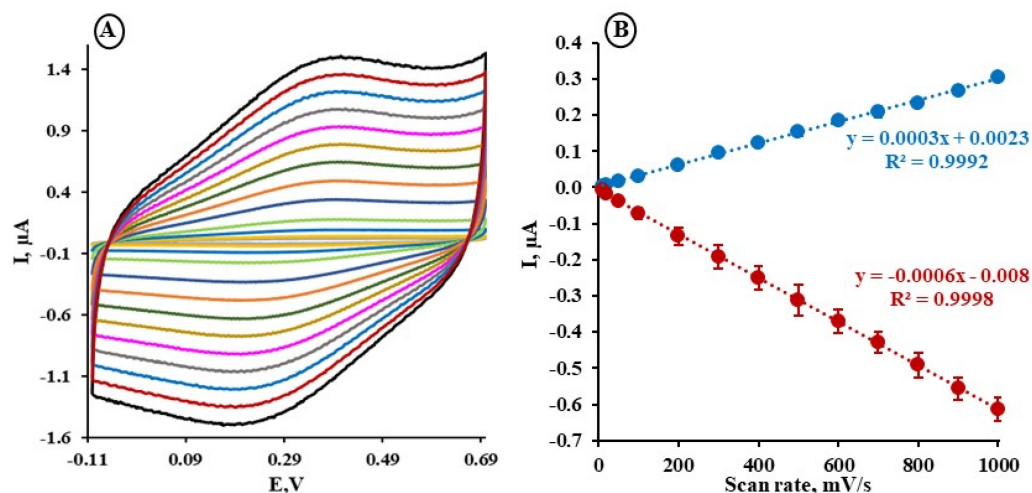


**Figure 1.** (A) An example of CV curves obtained for the gold electrode surface modified with MBL, AHT/TPY/Co(II)/DPM-AR layer, (B) plot of ( $\bullet$ ,  $I_{pa}$ ) anodic and ( $\bullet$ ,  $I_{pc}$ ) cathodic peak current vs. potential scan rate (0.050–1.0 V/s). Buffer composition: 0.1 M NaNO<sub>3</sub> + 0.01 M H<sub>3</sub>BO<sub>3</sub> at pH 4.0.

The number of anion receptor molecules deposited on the gold electrode surface could be estimated based on the quantity of charge involved in the Co(III)/Co(II) reduction processes registered in CV. Surface coverage ( $\Gamma$ ) of redox-active centers was calculated based on Equation (S4) (Supplementary Materials) [28] and is  $2.4 \pm 9.5 \times 10^{-11}$  mol/cm<sup>2</sup>. As expected, this value is in a similar range as calculated for analogous systems in our previous work [29].

The values of the electron transfer coefficient ( $\alpha$ ) and the electron transfer rate constant ( $k_0$  [s<sup>-1</sup>]) for the Au/MBL, AHT/TPY/Co(II)/DPM-AR layer were calculated based on the generally applicable Laviron's formula (Equations (S5) and (S6), Supplementary Materials) and amounted to  $0.53 \pm 0.01$  and  $0.99 \pm 0.03$ , respectively. The value of  $\alpha$  is close to 0.5, indicating an equal share of the total free energy of activation for electron transfer between the anodic and cathodic steps [30,31].

### 2.3. The Electrochemical Detection of Chloride Using the Au/MBL, AHT/TPY/Co(II)/DPM-AR layer

The electrochemical detection of chloride using the Au/MBL, AHT/TPY/Co(II)/DPM-AR layer was carried out based on SWV experiments. The gold electrode modified with the MBL, AHT/TPY/Co(II)/DPM-AR layer was characterized by the peak current and position of 0.78  $\mu$ A and 410 mV, respectively, registered in 0.1 M NaNO<sub>3</sub> + 0.01 M H<sub>3</sub>BO<sub>3</sub> at pH 4.0 (Figure 2A, dashed black line). Initially, the concentration range of the system response towards Cl<sup>-</sup> was optimized to acquire optimal analytical parameters for the presented system [23,24]. The procedure of optimizing the concentration range was started from conducting experiments of detection of the chloride anions by the system proposed in the pM concentration range. However, due to the large decrease in the current caused by the interaction of Cl<sup>-</sup> with DPM-AR in this concentration range, in the next steps, the concentration range was lowered by one order of magnitude at a time until the system showed a linear change in the  $\Delta I$  ( $\mu$ A) vs. log C (M). Finally, the concentration range between 1 and 45 fM was selected for the study of these interactions.

When the MBL, AHT/TPY/Co(II)/DPM-AR modified gold electrodes were in contact with growing concentrations of Cl<sup>-</sup> (Figure 2A), a gradual decrease in the relative Co(II)/Co(III) peak current intensity was observed up to  $\Delta I$  equal about  $-0.41 \pm 0.01$   $\mu$ A (Figure 2D). The current decrease was assisted by a peak potential shift towards lower values. For the highest concentration of chloride (45 fM), the potential shift was  $-48.6 \pm 2.3$  mV (Figure S1, Supplementary Materials). A similar phenomenon, namely a cathodic shift  $\Delta E$  [mV] of the redox-active anion receptor upon anion binding, was observed by other authors [15].

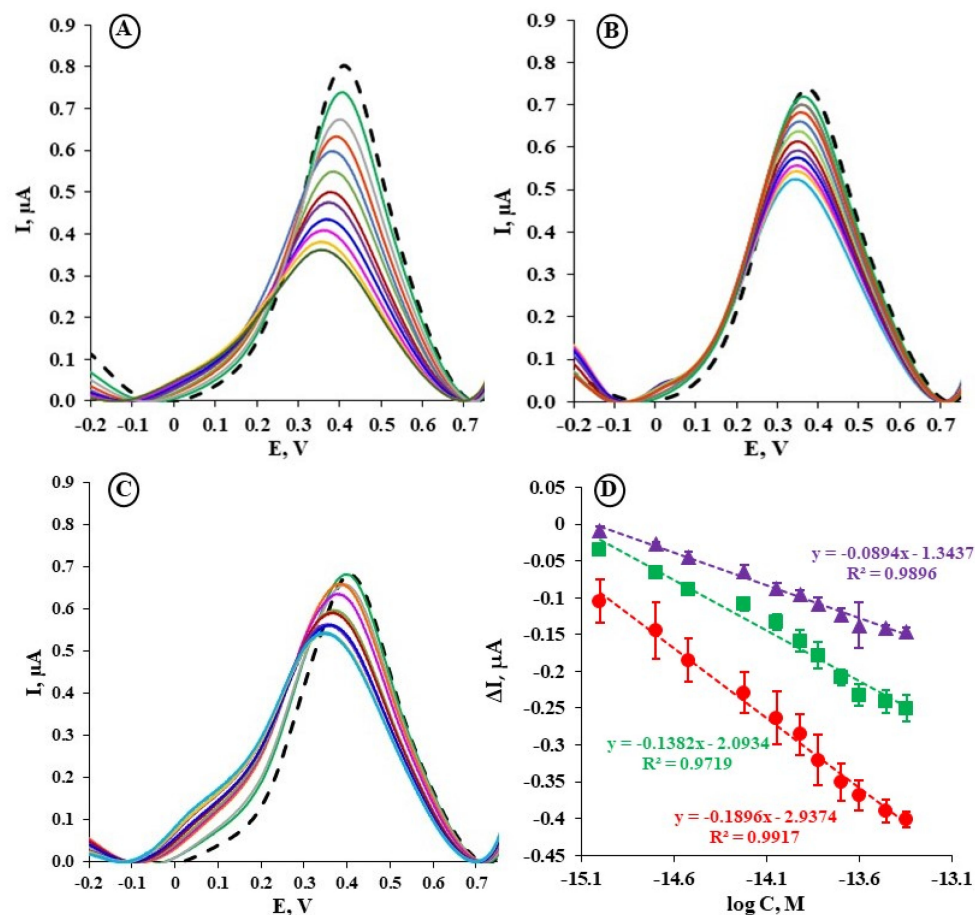


**Figure 2.** Representative SWVs recorded for the Au/MBL, AHT/TPY/Co(II)/DPM-AR layer in the presence of (A) chloride, (B) sulfate and (C) bromide in 0.1 M  $\text{NaNO}_3$  + 0.01 M  $\text{H}_3\text{BO}_3$  at pH 4.0. (D) Redox current differences  $\Delta I = I_n - I_0$ ,  $\mu\text{A}$  for the Au/MBL, AHT/TPY/Co(II)/DPM-AR in the presence of (●) chloride, (■) sulfate and (▲) bromide in 0.1 M  $\text{NaNO}_3$  + 0.01 M  $\text{H}_3\text{BO}_3$  at pH 4.0 ( $n = 5 \div 6$ ).

The selectivity of the sensor is an important factor influencing its analytical performance. To evaluate the selectivity of this layer, the two target anions, sulfate and bromide, were tested separately under the same conditions. Significantly smaller decreases in the Co(II)/Co(III) peak current, compared to  $\text{Cl}^-$ , were observed for the Au/MBL, AHT/TPY/Co(II)/DPM-AR upon interaction with 45 fM of  $\text{SO}_4^{2-}$  and  $\text{Br}^-$ , up to  $-0.25 \mu\text{A} \pm 0.02$  and  $-0.14 \pm 0.01 \mu\text{A}$ , respectively (Figure 2B,C). Additionally, the shift of the potential for sulfate and bromide was similar, about  $-23 \text{ mV}$  (Figure S1, Supplementary Materials), which is approximately two times smaller than for chloride. An additional parameter determined the selectivity of the sensor—the response ratio  $R_{i,j}$  was calculated according to Equation (S7) (Supplementary Materials). The low values of  $R_{i,j}$  (below 1.0) of 0.73 and 0.47 (Supplementary Materials, Table S1) for interfering anions showed that the selectivity of chloride towards sulfate and bromide is very high [32]. The selectivity factor  $\alpha_f$  of the proposed sensor was estimated by Equation (S8) (Supplementary Materials) to be equal to 2.1 ( $\text{SO}_4^{2-}$ ) and 3.9 ( $\text{Br}^-$ ) [33].

The mechanism of the high selectivity for  $\text{Cl}^-$  anions is related to the higher binding constant of  $\text{Cl}^-$  with the anion receptor. The corresponding thiourea derivatives are known as effective receptors for chloride [34]. The complexation of the chloride to the anion receptor influences the redox reaction of the cobalt redox center. Different possible pathways of the reaction coupling realization include those through space electrostatic interaction between redox centers and complexed anions, bond communication, or conformational changes of the redox centers influenced by the complexation process. All these possible

phenomena could cause changes in electron transfer efficiency to/from the electrode and reflect the reaction coupling efficiency (RCE) [16].

The linear relationships between the relative values of the current decrease of Co(II)/Co(III) peak current and concentration of chloride ions were observed over the entire range of analyzed chloride, from 1 to 45 fM (Figure 2D). On the other hand, the LOD was calculated using Equation (S9) and was equal to 0.50 fM (Supplementary Materials) [35].

Over the last decade, a few reports on the electrochemical detection of chloride anions in aqueous environments have been published in the scientific literature [18–23,36–40]. Some examples collected in Table 1 clearly show that the presented system has better sensitivity (fM range) than most of the literature references. The LODs of most sensors displayed in Table 1 are in the micromolar or lower range for chloride determinations. Only one example, which is based on a redox-active receptor deposited on the gold electrode surface, allowing for the determination of  $\text{Cl}^-$  in the pM range in aqueous solutions, has been presented till now [23]. Our results clearly show that changing the dipyrromethene to terpyridine to form a redox-active complex with Co(II) improved the LOD of  $\text{Cl}^-$  by almost three orders of magnitude. This system is based on a bifunctional receptor molecule that contains two elements in one, namely binding sites of AR and a TPY/Co(II)/DPM redox-active center. The electron transfer reactions of the redox centers are coupled with the complexation reactions of the receptor (Scheme 2). The specific mechanism is worth further exploration. However, there are some possible explanations that could be related to the differences in thermodynamically important stability constant of complexes TPY/Co(II)/DPM or DPM/Co(II)/DPM or the differences in the conformational induced perturbation of redox centers caused by the complexation of the anion to the anion receptor [16]. Moreover, it has been reported that terpyridines are  $\pi$ -acceptors and stabilize the metals in a lower oxidation state, which could be an additional motive for the difference in the obtained LOD in both cases.

The association constant ( $K_A$ ) of the AR with chloride was calculated using a Langmuir isotherm approach [29] and was found to be  $2.78 \pm 0.21 \times 10^{13} \text{ M}^{-1}$ . This approach is based on the linearization of the Langmuir isotherm, according to Equation (S10). The linear relationship of  $(I_n - I_0)/I_0$  vs.  $C [M]$  is shown in Figure S2, Supplementary Materials. Hence, the affinity interaction between AR and chloride ions was described by a dissociation constant  $K_D$  of  $6.13 \pm 0.45 \times 10^{-14} \text{ M}$  (Equation (S11), Supplementary Materials). Then, the thermodynamic parameter  $\Delta G$  (change in Gibb's free energy) using Van 't Hoff (Equation (S12), Supplementary Materials) [41] was calculated and was equal to  $-69.6 \pm 2 \text{ kJ/mol}$ , which means spontaneous interaction of anion receptor and chloride (Table S2, Supplementary Materials).

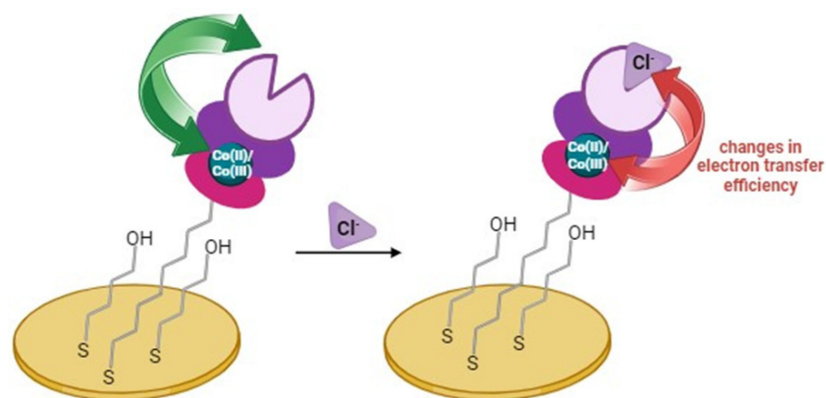
Interfacial binding constants ( $K$ ) for the formation of complexes of the target anions with the AR were also estimated. The detailed procedure for these calculations is demonstrated in the Supplementary Materials (Equation (S13), Figure S3) [42]. The obtained results clearly show that the affinity for chloride ( $20 \times 10^{13} \text{ M}^{-1}$ ) is the strongest, and the values of the sulfate ( $5.13 \times 10^{13} \text{ M}^{-1}$ ) and bromide ( $2.13 \times 10^{13} \text{ M}^{-1}$ ) binding constants were an order of magnitude lower (Table S3). The explanation for such high binding constants ( $K$ ) is the fact that the anion recognition process occurs at the interface between the aqueous solution and the modified electrode surface [23].

The reaction coupling efficiency parameter ( $RCE$ ) is the next factor, which was calculated to support and confirm the obtained results. It provides information about the effectiveness of anion binding to the receptor, calculated according to Equation (S14) (Supplementary Materials) [43]. CV curves recorded at anion concentrations of 0 and 15 fM were selected to calculate the  $RCE$  parameter. The obtained  $RCE$  values are  $5.2 \pm 0.5$ ,  $2.3 \pm 0.6$ , and  $1.3 \pm 0.3$  for chloride, sulfate and bromide, respectively (Table S3). The  $RCE$  value for  $\text{Cl}^-$  is higher than for  $\text{SO}_4^{2-}$  and  $\text{Br}^-$ , which indicates that chloride complexation is more efficient [23].

**Table 1.** Comparison of electrochemical sensors for detection of chloride anions in aquatic media (last decade).

Sensor	Method	LOD, M	Interferents	Ref.
GPE/AgNPs	CV	$4.1 \times 10^{-5}$	$\text{CO}_3^{2-}$ , $\text{NO}_3^-$ , $\text{NO}_2^-$ , $\text{PO}_4^{3-}$ , $\text{SO}_4^{2-}$	[36]
CD/Ag	LSV	$2 \times 10^{-5}$	$\text{NO}_2^-$ , $\text{PO}_4^{2-}$ , $\text{Na}^+$ , $\text{K}^+$ , $\text{SO}_4^{2-}$	[18]
PTFE/MWCNT/(Ag-NPs/AgCl)/Cu-BTC	ChA	nd	$\text{NO}_3^-$ , $\text{SO}_4^{2-}$ , $\text{S}^{2-}$ , $\text{OH}^-$	[19]
GCE/ZIF-8/AgNPs	DPV	$6.1 \times 10^{-7}$	$\text{NO}_3^-$ , $\text{SO}_4^{2-}$ , $\text{CO}_3^{2-}$ , $\text{PO}_4^{2-}$	[20]
ISE/TCNQ-TTF/CB	Pm	$2.51 \times 10^{-6}$	$\text{NO}_3^-$ , $\text{NO}_2^-$ , $\text{SO}_4^{2-}$ , $\text{CO}_3^{2-}$ , $\text{HCO}_3^-$ , $\text{CH}_3\text{COO}^-$	[37]
FP/Ag Ink	CV	$1 \times 10^{-3}$	$\text{HPO}_4^{2-}$ , $\text{H}_2\text{PO}_4^{2-}$ , $\text{CO}_3^{2-}$ $\text{HCO}_3^-$ , $\text{Br}^-$ , $\text{I}^-$ , $\text{CN}^-$	[38]
OP/Ag Ink	CV	$7 \times 10^{-6}$	nd	[39]
ISE/PDMS/AgNWs	Vm	$5 \times 10^{-4}$	$\text{HCO}_3^-$ , $\text{CO}_3^{2-}$ , $\text{OH}^-$ , $\text{NO}_3^-$	[40]
CSPE/FcMeOH CSPE/ $\text{K}_4[\text{Fe}(\text{CN})_6]$ CSPE/ $\text{K}_3[\text{Fe}(\text{CN})_6]$	DPV	0.01 2 2	$\text{AsO}_4^{2-}$ , $\text{PO}_4^{3-}$ , $\text{I}^-$ , $\text{CN}^-$ , $\text{Br}^-$ , $\text{CO}_3^{2-}$ , $\text{CrO}_4^{2-}$ , $\text{Cr}_2\text{O}_7^{2-}$ , $\text{IO}_3^-$ , $\text{BrO}_3^-$ , $\text{SO}_4^{2-}$ , $\text{Hg}_2^{2+}$ , $\text{Pb}^{2+}$	[21]
CSPE/Gore-Tex/FcMeOH	DPV	$2 \times 10^{-4}$	nd	[22]
Au/DPM/Cu(II)/DPM-AR Au/DPM/Co(II)/DPM-AR	SWV	$1.0 \times 10^{-12}$ $1.1 \times 10^{-12}$	$\text{SO}_4^{2-}$ , $\text{Br}^-$	[23]
Au/AHT,MBL/TPY/Co(II)/DPM-AR	SWV	$5.0 \times 10^{-16}$	$\text{SO}_4^{2-}$ , $\text{Br}^-$	This work

Abbreviations: GPE—graphite pencil electrode, AgNPs—silver nanoparticles, GPE—graphite pencil electrode, CD—compact discs, LSV—linear scan voltammetry, PTFE—flexible polytetrafluoroethylene, MWCNT—multiwalled carbon nanotubes, Cu-BTC—hydrophilic copper benzene-1,3,5-tricarboxylate, ChA—chronoamperometry, nd—not determined, ZIF—zeolitic imidazolate framework, DPV—differential pulse voltammetry, ISE—ion-selective electrode, TCNQ-TTF—tetrathiafulvalene-tetracyanoquinodimethane, CB—carbon black, Pm—potentiometry, FP—filter paper, CV—cyclic voltammetry, OP—office paper, PDMS—composite of polydimethylsiloxane, AgNWs—silver nanowires, Vm—voltammetry, CSPE—carbon screen-printed electrode, FcMeOH—ferrocenemethanol, Gore-tex—laminated waterproof breathable ripstop nylon fabric, DPM-AR dipyrromethene-anion receptor, AHT—aminohexanethiol, MBL—mercaptobutanol, TPY—terpyridine, SWV—square wave voltammetry.

**Scheme 2.** Schematic representation of the sensing principle.

#### 2.4. The Repeatability, Reproducibility and Stability of the Sensing Layer

The sensing layer of Au/MBL, AHT/TPY/Co(II)/DPM-AR was also characterized by repeatability, reproducibility and stability over time. Repeatability and reproducibility were then assessed with relative standard deviations (RSD) of 2.9% and 4.7%, respectively (Figure 3A). The stability of the sensor was examined by recording SWV curves in the presence of  $\text{Cl}^-$  anions in the concentration range from 1 fM to 45 fM after 7 days of storing gold electrodes modified with TPY/Co(II)/DPM-AR at 4 °C. Stability studies show that after 7 days of storage, the sensor response decreases by ~9.5% (Figure 3B).

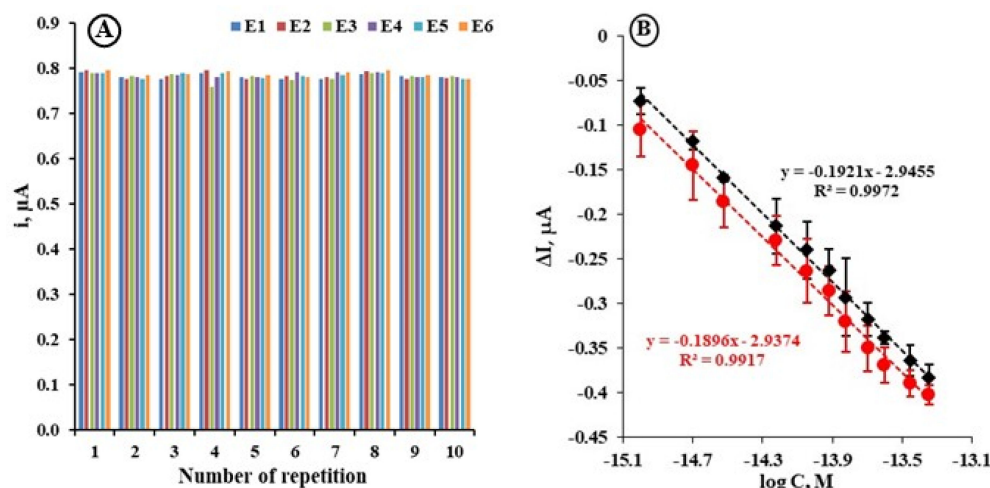


**Figure 3.** (A) Results of repeatability and reproducibility studies obtained for the gold electrode surface modified with the MBL, AHT/TPY/Co(II)/DPM-AR in 0.1 M  $\text{NaNO}_3$  + 0.01 M  $\text{H}_3\text{BO}_3$  at pH 4.0. (B) Redox current differences  $\Delta I = I_n - I_0$ ,  $\mu\text{A}$  recorded using SWV for Au/MBL,AHT/TPY-Co(II)/DPM-AR in the presence of (●) chloride measured directly after modification and (◆) chloride measured 7 days of storage at 4 °C in 0.1 M  $\text{NaNO}_3$  + 0.01 M  $\text{H}_3\text{BO}_3$  at pH 4.0 ( $n = 3$ ).

### 3. Materials and Methods

#### 3.1. Materials

The DPM-AR (Scheme 1B) and the terpyridine-NHS (TPY-NHS) were synthesized at the Department of Chemistry, KU Leuven, Leuven. The procedure for synthesis was briefly described in the Supplementary Materials (Scheme S1) [23]. AHT, MBL, cobalt (II) acetate  $\text{Co}(\text{OAc})_2$ , dichloromethane (DCM), sodium chloride (NaCl), sodium sulfate ( $\text{Na}_2\text{SO}_4$ ), sodium bromide (NaBr), sodium nitrate ( $\text{NaNO}_3$ ) and boric acid ( $\text{H}_3\text{BO}_3$ ) were purchased from Sigma-Aldrich (Poznań, Poland). Potassium hydroxide (KOH), sulfuric acid ( $\text{H}_2\text{SO}_4$ ), nitric acid ( $\text{HNO}_3$ ) and methanol (MeOH) were obtained from Avantor Performance Materials (Gliwice, Poland). All reagents were of analytical grade. All aqueous solutions were prepared with deionized and charcoal-treated water (resistivity of 18.2  $\text{M}\Omega \text{ cm}$ ) purified with a Milli-Q reagent grade water system (Millipore, Bedford, MA, USA). These solutions were deoxygenated by purging with nitrogen (ultrapure 6.0, Air Products, Warszawa, Poland) for 15 min.

#### 3.2. Electrochemical Measurements

All electrochemical measurements were performed with a potentiostat-galvanostat AutoLab (Eco Chemie, Utrecht, The Netherlands) with a three-electrode configuration system. Potentials were measured vs. a silver chloride (Ag/AgCl) electrode, and a platinum wire was used as an auxiliary electrode. The voltammetric experiments were carried out in an electrochemical cell with a 10 mL volume. CV measurements were performed in the potential window from  $-100$  mV to 700 mV with different scan rates: 10, 20, 50, 100, 200, 300, 400, 500, 600, 700, 800, 900 and 1000  $\text{mV}\cdot\text{s}^{-1}$ . SWV was performed with a potential from  $-100$  mV to 700 mV with a step potential of 1 mV, a square wave frequency of 50 Hz, and an amplitude of 50 mV.

All measurements were conducted in the presence of an aqueous solution of 0.1 M  $\text{NaNO}_3$  and 0.01 M  $\text{H}_3\text{BO}_3$  (pH 4.0) as a supporting electrolyte. The influence of the pH on the response of this system in both the absence and presence of  $\text{Cl}^-$  anion was studied by varying the pH of the supporting electrolyte (0.1 M  $\text{NaNO}_3$  + 0.01 M  $\text{H}_3\text{BO}_3$ ) in a 4.0–7.0 range. The results showed that well-defined quasi-reversible peaks for Co(II)/Co(III) were obtained at pH 4.0. The reversibility of the redox reaction and the peak current decrease with an increase in the pH of the solution. Furthermore, at pH 4.0 the tertiary nitrogen atom of the anion receptor is protonated causing a stronger electrostatic interaction

between the anion receptor and the selected anions ( $\text{Cl}^-$ ,  $\text{SO}_4^{2-}$ , and  $\text{Br}^-$ ). Therefore, in order to get a stronger response and sensitivity of the sensing system, pH 4.0 was chosen as the optimum pH value for all the experiments [23]. Sensing experiments were carried out by adding target anions to the electrochemical cell. The measuring conditions for chloride recognition were experimentally selected in our previous work [23]. The analytical signal of the electrode was expressed as:  $\Delta I = I_n - I_0$ , where  $I_n$  is the peak current measured in the presence of the particular concentration of the analyte (anion) and  $I_0$  is the peak current before adding the analyte to the pure supporting electrolyte.

### 3.3. Fabrication of Sensing Layer for Detection of Chloride

Gold disk electrodes with a diameter of 2 mm (Bioanalytical Systems (BASi), West Lafayette, IN, USA) were used for all experiments. The preparation of gold electrode surfaces was performed according to an already published protocol [44]. Briefly, these electrodes were initially manually polished with alumina slurries (0.3  $\mu\text{m}$  and 0.05  $\mu\text{m}$ , Alpha and Gamma Micropolish, Buehler; Lake Bluff, IL, USA). The polished electrodes were then electrochemically cleaned by CV in 0.5 M KOH and then in 0.5 M  $\text{H}_2\text{SO}_4$ . Before modification, the electrode surfaces were refreshed with 0.5 M KOH. After electrochemical pre-treatment, each electrode was rinsed with Milli-Q water and kept in water (for a few minutes until the next step) to avoid air contamination. Immediately after cleaning, the electrodes were repeatedly rinsed with Milli-Q water, MeOH, and a mixture of MeOH and DCM (volume ratio 1:1) and immersed in modification solutions. Preparation of the layer has been illustrated in Scheme 1A and is as follows:

1. The gold electrodes were immersed in a mixture of 0.01 mM AHT and 1 mM MBL—3 h at room temperature (RT), DCM:MeOH (1:1, *v/v*); after modification, electrodes were carefully rinsed with a mixture of DCM:MeOH;
2. The reaction between the amine groups of AHT and NHS of 0.1 mM TPY-NHS during 1 h, RT, DCM:MeOH (1:1); after this step, electrodes were carefully washed with a mixture of DCM:MeOH;
3. The complexation of Co(II) ions was achieved by immersing electrodes in 1 mM of  $\text{Co}(\text{OAc})_2$ —1 h, RT, DCM:MeOH (1:1); after modification, electrodes were carefully rinsed with a mixture of DCM:MeOH;
4. The coordination sphere of the Co(II) metal ions was closed by 0.1 mM DPM-AR—1 h, RT, DCM-MeOH (1:1); after modification, electrodes were carefully washed with: a mixture of DCM:MeOH, MeOH, Milli-Q water, and 0.1 M  $\text{NaNO}_3$  + 0.01 M  $\text{H}_3\text{BO}_3$  pH 4.0 buffer and stored for approximately 36 h in the same buffer at 4 °C.

## 4. Conclusions

For some time now, electroactive self-assembled monolayers based on various receptors and metals, including dipyrromethenes, have been at the center of our interest [29]. According to our experience, the mixed monolayer of MBL and AHT is well organized and it is efficient for immobilization of terpyridine and complexation with Co(II), followed by closing the coordination sphere by dipyrromethene. Both terpyridines and dipyrromethenes are suitable molecules for creating complexes with transition metal ions. It was reported that terpyridines are  $\pi$ -acceptors and stabilize the metals in a lower oxidation state. These parameters may possibly affect the stability of the entire layer. Our results clearly show that the complex remains stable after an appropriate time of conditioning (7 days of storing).

The presented electrochemical anion sensing platform contains a chloride-binding receptor as an anion recognition element and a redox-active TPY/Co(II)/DPM complex immobilized on a gold electrode surface. The electrochemical characterization of this sensing layer was assessed using the following electrochemical parameters: electron transfer rate constant ( $k_0$ ), electron transfer coefficient ( $\alpha$ ) and surface coverage ( $\Gamma$ ).

The sensor under study enabled sensitive and selective detection of chloride in the fM range in an aqueous medium with a LOD of 0.50 fM. The selectivity of the sensor was

evidenced not only by the significantly lower voltammetric response of the sensor to sulfate and bromide but also by an additional parameter: namely, the response ratio,  $R_{ij}$ .

Furthermore, the lack of the need to use an external redox marker makes the sensor more attractive in terms of application and miniaturization. These features make the developed system an interesting analytical tool for monitoring chloride content in the environment.

**Supplementary Materials:** The following supporting information can be downloaded at: <https://www.mdpi.com/article/10.3390/molecules29092102/s1>, Table S1: Response ratio  $R_{ij}$  of Au/MBL+AHT/TPY-Co(II)/DPM-AR, Figure S1: Redox potential differences  $\Delta E = E_n - E_0$ , mV recorded using SWV for Au/MBL,AHT/TPY/Co(II)/DPM-AR in the presence of chloride. Table S2: The association constant  $K_A$ , dissociation constant  $K_D$  and Gibbs free energy  $\Delta G$  calculated for gold electrode modified with TPY/Co(II)/DPM-AR. Figure S2: The linear relationship of  $I_n - I_0/I_0$  vs.  $C_{Cl^-}$  [M] for TPY/Co(II)/DPM-AR modified gold electrode surface. Table S3: Binding constant ( $K$ ) and Reaction Coupling Efficiency ( $RCE$ ) of TPY/Co(II)/DPM-AR towards chloride, sulfate and bromide ( $n = 5$ ). Figure S3: Relationship of  $\exp\{\Delta E^{\circ'}(-nF/RT)\} - 1$  vs. concentration of (●) chloride, (■) sulfate and (▲) bromide. Description of anion receptor synthesis. Scheme S1: Synthesis of the dipyrromethene modified dipodal anion receptor.

**Author Contributions:** K.M.-B.—data curation, investigation, formal analysis, writing—original draft preparation, review and editing; M.D.—investigation; W.D.—conceptualization, writing—review and editing; H.R.—conceptualization, methodology; J.R.—funding acquisition, project administration, conceptualization, supervision; I.G.—data curation, writing—original draft preparation, review and editing. All authors have read and agreed to the published version of the manuscript.

**Funding:** This work was supported by the project of the National Science Centre, Poland, No. 2016/21/B/ST4/03834.

**Institutional Review Board Statement:** Not applicable.

**Informed Consent Statement:** Not applicable.

**Data Availability Statement:** Data will be made available on request.

**Acknowledgments:** This article is based upon work from COST Action LUCES, CA22131 supported by COST (European Cooperation in Science and Technology).

**Conflicts of Interest:** The authors declare no conflicts of interest.

## References

1. Beer, P.D.; Gale, P.A. Anion Recognition and Sensing: The State of the Art and Future Perspectives. *Angew. Chem. Int. Ed.* **2001**, *40*, 486–516. [CrossRef]
2. Kubik, S. Anion recognition in water. *Chem. Soc. Rev.* **2010**, *39*, 3648–3663. [CrossRef]
3. Langton, M.J.; Serpell, C.J.; Beer, P.D. Anion Recognition in Water: Recent Advances from a Supramolecular and Macromolecular Perspective. *Angew. Chem. Int. Ed.* **2016**, *55*, 1974–1987. [CrossRef]
4. Sessler, J.L.; Gale, P.; Cho, W.-S. Receptors for Ion-Pairs. In *Anion Receptor Chemistry*; Sessler, J.L., Gale, P.A., Cho, W.-S., Rowan, S.J., Aida, T., Rowan, A.E., Stoddart, J.F., Eds.; The Royal Society of Chemistry: London, UK, 2006.
5. Pal, A.; Karmakar, M.; Bhatta, S.R.; Thakur, A. A detailed insight into anion sensing based on intramolecular charge transfer (ICT) mechanism: A comprehensive review of the years 2016 to 2021. *Coord. Chem. Rev.* **2021**, *448*, 214167. [CrossRef]
6. McNaughton, D.A.; Fares, M.; Picci, G.; Gale, P.A.; Caltagirone, C. Advances in fluorescent and colorimetric sensors for anionic species. *Coord. Chem. Rev.* **2021**, *427*, 213573. [CrossRef]
7. Hein, R.; Beer, P.D.; Davis, J.J. Electrochemical Anion Sensing: Supramolecular Approaches. *Chem. Rev.* **2020**, *120*, 1888–1935. [CrossRef] [PubMed]
8. Xue, Y.; Zheng, Y.; Wang, E.; Yang, T.; Wang, H.; Hou, X.  $Ti_3C_2T_x$  (MXene)/Pt nanoparticle electrode for the accurate detection of DA coexisting with AA and UA. *Dalton Trans.* **2022**, *51*, 4549–4559. [CrossRef]
9. Jia, D.; Yang, T.; Wang, K.; Zhou, L.; Wang, E.; Chou, K.-C.; Wang, H.; Hou, X. Facile in-situ synthesis of  $Ti_3C_2T_x/TiO_2$  nanowires toward simultaneous determination of ascorbic acid, dopamine and uric acid. *J. Alloys Compd.* **2024**, *985*, 173392. [CrossRef]
10. Li, G.; Qi, X.; Wu, J.; Wan, X.; Wang, T.; Liu, Y.; Chen, Y.; Xia, Y. Highly stable electrochemical sensing platform for the selective determination of pefloxacin in food samples based on a molecularly imprinted-polymer-coated gold nanoparticle/black phosphorus nanocomposite. *Food Chem.* **2024**, *436*, 137753. [CrossRef]

11. Li, G.; Wu, J.; Qi, X.; Wan, X.; Liu, Y.; Chen, Y.; Xu, L. Molecularly imprinted polypyrrole film-coated poly(3,4-ethylenedioxythiophene):polystyrene sulfonate-functionalized black phosphorene for the selective and robust detection of norfloxacin. *Mater. Today Chem.* **2022**, *26*, 101043. [[CrossRef](#)]
12. Wan, X.; Du, H.; Tuo, D.; Qi, X.; Wang, T.; Wu, J.; Li, G. UiO-66/Carboxylated Multiwalled Carbon Nanotube Composites for Highly Efficient and Stable Voltammetric Sensors for Gatifloxacin. *ACS Appl. Nano Mater.* **2023**, *6*, 19403–19413. [[CrossRef](#)]
13. Zhao, J.; Yang, D.; Yang, X.-J.; Wu, B. Anion coordination chemistry: From recognition to supramolecular assembly. *Coord. Chem. Rev.* **2019**, *378*, 415–444. [[CrossRef](#)]
14. Khurana, R.; Alami, F.; Nijhuis, C.A.; Keinan, E.; Huskens, J.; Reany, O. Selective Perchlorate Sensing Using Electrochemical Impedance Spectroscopy with Self-Assembled Monolayers of semiaza-Bambusurils. *Chem. A Eur. J.* **2024**, *30*, e202302968. [[CrossRef](#)] [[PubMed](#)]
15. Hein, R.; Li, X.; Beer, P.D.; Davis, J.J. Enhanced voltammetric anion sensing at halogen and hydrogen bonding ferrocenyl SAMs. *Chem. Sci.* **2021**, *12*, 2433–2440. [[CrossRef](#)] [[PubMed](#)]
16. Beer, P.D.; Gale, P.A.; Chen, G.Z. Mechanisms of electrochemical recognition of cations, anions and neutral guest species by redox-active receptor molecules. *Coord. Chem. Rev.* **1999**, *185–186*, 3–36. [[CrossRef](#)]
17. Ke, X. Micro-fabricated electrochemical chloride ion sensors: From the present to the future. *Talanta* **2020**, *211*, 120734. [[CrossRef](#)] [[PubMed](#)]
18. Patella, B.; Aiello, G.; Drago, G.; Torino, C.; Vilasi, A.; O’Riordan, A.; Inguanta, R. Electrochemical detection of chloride ions using Ag-based electrodes obtained from compact disc. *Anal. Chim. Acta* **2022**, *1190*, 339215. [[CrossRef](#)] [[PubMed](#)]
19. Kwak, B.; Park, S.; Lee, H.S.; Kim, J.; Yoo, B. Improved Chloride Ion Sensing Performance of Flexible Ag-NPs/AgCl Electrode Sensor Using Cu-BTC as an Effective Adsorption Layer. *Front. Chem.* **2019**, *7*, 637. [[CrossRef](#)] [[PubMed](#)]
20. Bin, Q.; Wang, M.; Wang, L. Ag nanoparticles decorated into metal-organic framework (Ag NPs/ZIF-8) for electrochemical sensing of chloride ion. *Nanotechnology* **2020**, *31*, 125601. [[CrossRef](#)]
21. Bujes-Garrido, J.; Arcos-Martínez, M.J. Disposable sensor for electrochemical determination of chloride ions. *Talanta* **2016**, *155*, 153–157. [[CrossRef](#)]
22. Bujes-Garrido, J.; Arcos-Martínez, M.J. Development of a wearable electrochemical sensor for voltammetric determination of chloride ions. *Sens. Actuators B Chem.* **2017**, *240*, 224–228. [[CrossRef](#)]
23. Kaur, B.; Erdmann, C.A.; Daniëls, M.; Dehaen, W.; Rafiński, Z.; Radecka, H.; Radecki, J. Highly Sensitive Electrochemical Sensor for the Detection of Anions in Water Based on a Redox-Active Monolayer Incorporating an Anion Receptor. *Anal. Chem.* **2017**, *89*, 12756–12763. [[CrossRef](#)] [[PubMed](#)]
24. Malecka, K.; Menon, S.; Palla, G.; Kumar, K.G.; Daniels, M.; Dehaen, W.; Radecka, H.; Radecki, J. Redox-Active Monolayers Self-Assembled on Gold Electrodes—Effect of Their Structures on Electrochemical Parameters and DNA Sensing Ability. *Molecules* **2020**, *25*, 607. [[CrossRef](#)] [[PubMed](#)]
25. Wu, D.; Hu, Y.; Liu, Y.; Zhang, R. Review of Chloride Ion Detection Technology in Water. *Appl. Sci.* **2021**, *11*, 11137. [[CrossRef](#)]
26. Zaki, M.H.M.; Mohd, Y.; Chin, L.Y. Surface Properties of Nanostructured Gold Coatings Electrodeposited at Different Potentials. *Int. J. Electrochem. Sci.* **2020**, *15*, 11401–11415. [[CrossRef](#)]
27. Xie, X.; Holze, R. Electrode Kinetic Data: Geometric vs. Real Surface Area. *Batteries* **2022**, *8*, 146. [[CrossRef](#)]
28. Bard, A.J.; Faulkner, L.R.; White, H.S. *Electrochemical Methods: Fundamentals and Applications*; John Wiley & Sons: Hoboken, NJ, USA, 2022.
29. Szymańska, I.; Stobiecka, M.; Orlewska, C.; Rohand, T.; Janssen, D.; Dehaen, W.; Radecka, H. Electroactive Dipyrromethene–Cu(II) Self-Assembled Monolayers: Complexation Reaction on the Surface of Gold Electrodes. *Langmuir* **2008**, *24*, 11239–11245. [[CrossRef](#)] [[PubMed](#)]
30. Laviron, E. General expression of the linear potential sweep voltammogram in the case of diffusionless electrochemical systems. *J. Electroanal. Chem. Interfacial Electrochem.* **1979**, *101*, 19–28. [[CrossRef](#)]
31. Eckermann, A.L.; Feld, D.J.; Shaw, J.A.; Meade, T.J. Electrochemistry of redox-active self-assembled monolayers. *Coord. Chem. Rev.* **2010**, *254*, 1769–1802. [[CrossRef](#)]
32. Maccà, C.; Wang, J. Experimental procedures for the determination of amperometric selectivity coefficients. *Anal. Chim. Acta* **1995**, *303*, 265–274. [[CrossRef](#)]
33. Amouzadeh Tabrizi, M.; Acedo, P. An Electrochemical Immunosensor for the Determination of Procalcitonin Using the Gold-Graphene Interdigitated Electrode. *Biosensors* **2022**, *12*, 771. [[CrossRef](#)]
34. Scholten, K.; Merten, C. Anion-binding of a chiral tris(2-aminoethyl)amine-based tripodal thiourea: A spectroscopic and computational study. *Phys. Chem. Chem. Phys.* **2022**, *24*, 4042–4050. [[CrossRef](#)]
35. Swartz, M.E.; Krull, I.S. (Eds.) *Analytical Method Development and Validation*, 1st ed.; CRC Press: Boca Raton, FL, USA, 1997.
36. Maarroof, Y.T.; Mahmoud, K.M. Silver nanoparticle-modified graphite pencil electrode for sensitive electrochemical detection of chloride ions in pharmaceutical formulations. *Bull. Chem. Soc. Ethiop.* **2023**, *37*, 491–503. [[CrossRef](#)]
37. Pięk, M.; Paczosa-Bator, B.; Smajdor, J.; Piech, R. Molecular organic materials intermediate layers modified with carbon black in potentiometric sensors for chloride determination. *Electrochim. Acta* **2018**, *283*, 1753–1762. [[CrossRef](#)]
38. Cinti, S.; Fiore, L.; Massoud, R.; Cortese, C.; Moscone, D.; Palleschi, G.; Arduini, F. Low-cost and reagent-free paper-based device to detect chloride ions in serum and sweat. *Talanta* **2018**, *179*, 186–192. [[CrossRef](#)] [[PubMed](#)]

39. de Araujo, W.R.; Paixão, T.R.L.C. Fabrication of disposable electrochemical devices using silver ink and office paper. *Analyst* **2014**, *139*, 2742–2747. [[CrossRef](#)] [[PubMed](#)]
40. Xu, G.; Cheng, C.; Yuan, W.; Liu, Z.; Zhu, L.; Li, X.; Lu, Y.; Chen, Z.; Liu, J.; Cui, Z.; et al. Smartphone-based battery-free and flexible electrochemical patch for calcium and chloride ions detections in biofluids. *Sens. Actuators B Chem.* **2019**, *297*, 126743. [[CrossRef](#)]
41. Sikarwar, B.; Singh, V.V.; Sharma, P.K.; Kumar, A.; Thavaselvam, D.; Boopathi, M.; Singh, B.; Jaiswal, Y.K. DNA-probe-target interaction based detection of *Brucella melitensis* by using surface plasmon resonance. *Biosens. Bioelectron.* **2017**, *87*, 964–969. [[CrossRef](#)]
42. Gobi, K.V.; Ohsaka, T. Anion recognition and electrochemical characteristics of the self-assembled monolayer of nickel(II) azamacrocyclic complex. *J. Electroanal. Chem.* **2000**, *485*, 61–70. [[CrossRef](#)]
43. Beer, P.D.; Gale, P.A.; Chen, Z. Electrochemical Recognition of Charged and Neutral Guest Species by Redox-active Receptor Molecules††Manuscript received 9th October 1995. In *Advances in Physical Organic Chemistry*; Bethell, D., Ed.; Academic Press: Cambridge, MA, USA, 1999; Volume 31, pp. 1–90.
44. Malecka-Baturo, K.; Żółtowska, P.; Jackowska, A.; Kurzątkowska-Adaszyńska, K.; Grabowska, I. Electrochemical Aptasensing Platform for the Detection of Retinol Binding Protein-4. *Biosensors* **2024**, *14*, 101. [[CrossRef](#)]

**Disclaimer/Publisher’s Note:** The statements, opinions and data contained in all publications are solely those of the individual author(s) and contributor(s) and not of MDPI and/or the editor(s). MDPI and/or the editor(s) disclaim responsibility for any injury to people or property resulting from any ideas, methods, instructions or products referred to in the content.